HYDROGEN FUEL CELL & ENERGY STORAGE

Simulation of integrated purification systems for hydrogen production in the methanol steam reforming process

H. Alitabar- Firuzjah[a] | V. Kord Firuzjaei[b] | E. Alizadeh[c,*] | M. Sedighi[b] | M. Rahimi-Esbo[d]

[a] M.Sc. Graduate, Research Lab for Advanced Separation Processes, School of Chemical, Petroleum, and Gas Engineering, Iran University of Science and Technology (IUST), Iran

[b] Researcher, Northern Research Center for Science & Technology, Malek Ashtar University of Technology, Iran.

[c] Associated professor, Faculty of Aerospace, Malek Ashtar University of Technology, Iran, Email: ealizadeh@mut.ac.ir

[d] Assistant professor, Northern Research Center for Science & Technology, Malek Ashtar University of Technology, Iran.

Article Information

Article Type:
Research Article

Article History:

Received: 12 June 2023
Received in revised form
2 Augest 2023
Accepted: 1 September 2023
Published on line 21 September 2023

Keywords

Methanol-Steam Reforming
Hydrogen production
Purification system
PSA process
Simulation

Abstract

Recently, the use of clean energy has become an interesting topic for researchers, with Hydrogen attracting the attention of researchers and industries as an alternative energy source. Among existing hydrogen production sources, methanol fuel is considered an attractive feedstock for hydrogen production due to its advantages. However, the output stream from a methanol steam reforming reactor contains some carbon monoxide, and considering that carbon monoxide leads to fuel cell catalyst damage, its concentration needs to be reduced. The present work focuses on the design and simulation of a purification system for the methanol steam reforming process. Therefore, in the present study, a PROX unit was used to reduce the concentration of carbon monoxide output in the reformer. In this system, Pt/Al_2O_3 catalyst was first used to increase the reaction rate. Then, Aspen plus V11.0 software was used to simulate the PROX system. Subsequent results showed that carbon monoxide was completely removed from the system in the reactor. Next, in order to increase the concentration of hydrogen, a pressure swing adsorption (PSA) column, including an activated carbon absorber, was used as a purification system. Simulation and design of the PSA process were done in Aspen adsorption V11.0 software. A hydrogen purity of 99.9915% was obtained in the output stream from the PSA column. To validate the results obtained from the simulation, the present work was compared with the study of Abdeljaoued et al. [30]. The study's simulation results showed an acceptable error percentage with the results of that article.

Cite this article: Alitabar- Firuzjah, H., Kord Firuzjaei,V., Alizadeh, E., Sedighi, M,. Rahimi-Esbo, M (2023). Simulation of integrated purification systems for hydrogen production in the methanol steam reforming process. DOI:10.22104/HFE.2023.6084.1258

Publisher:Iranian Research Organization for Science and Technology(IROST)
DOI: 10.22104/HFE.2023.6084.1258

1. Introduction

Hydrogen is one of the most important compounds in industry, and its importance as an alternative energy carrier has increased in recent years due to the depletion of fossil fuels and increasing environmental concerns[1, 2]. Hydrogen can be produced through various processes, such as natural gas reforming or biogas, gasification, water electrolysis, photo-electrolysis, and biological processes [3]. Among these processes mentioned, current hydrogen production on a large scale is usually achieved by two processes: fossil fuel reforming and water electrolysis, both of which are fully developed at industrial levels [4]. The reforming process includes steam reforming, partial oxidation, dry reforming, and autothermal reforming. Although steam methane reforming (SMR) is one of the oldest processes for producing hydrogen from methane [5, 6], at this time, natural gas steam reforming is more cost-effective and efficient than methanol steam reforming for hydrogen production. Although methane steam reforming can be a suitable alternative to methanol economically, it is not a good solution for hydrogen production in the long term because natural gas reforming requires a high operating temperature, which produces a large amount of carbon dioxide [7, 8]. In general, methanol has a high H/C ratio (about 3-4) and unlike hydrocarbon fuels, methanol is free of any sulfur compounds [9]. Therefore, this fuel doesn't need any additional equipment (such as desulfurization and pre-reforming). Also, the reforming process related to methanol is done at a temperature of about 200-300 °C [3], with methanol, water, carbon monoxide, carbon dioxide, and hydrogen as products of the methanol steam reforming process [10].

If the purpose of hydrogen production is to use it in fuel cells, the amount of CO in the product stream should be minimal (less than 10 ppm) [11] because CO poisons the platinum anode catalyst. Among the various methods to reduce the concentration of carbon monoxide, preferential oxidation of carbon monoxide (PROX) is the simplest and most economical method, with the output stream from methanol steam reforming including an insignificant concentration of CO (less than 1mole percent) [12].

In recent years, various works have been done in the field of methanol steam reforming process using different catalysts. For example, an integrated system for hydrogen production via autothermal reforming of methanol as a fuel in a polymer electrolyte membrane (PEM) fuel cell, including an autothermal reforming reactor, a preferential oxidation reactor (PROX), and a fuel cell, was designed and investigated by Ouzounidou et al. [13]. In this work, a CuO/CeO_2 catalyst, at the temperature of 200.5℃, and an O_2/CO ratio of 1 to 5 resulted in about a 98% removal of carbon monoxide [13]. Other studies have investigated the best conditions for achieving a high conversion percentage of methanol and removing carbon monoxide from the system by studying operational parameters (i.e., operating temperature, the ratio of oxygen to carbon monoxide, and reactor length) [14, 15]. The catalysts of the preferential CO oxidation process are divided into three main groups: Noble metals catalysts, such as Pt, Pd, Ir, Ru, and Rh supported by mainly alumina oxide, are used as metal oxide. When the operating temperature is less than 100 ℃, the combination of a gold catalyst with metal oxides such as iron or magnesium is a very suitable catalyst. When the operating temperature is between 170-190°C, a CuO/CeO_2 combination is the most suitable catalyst, with both high selectivity and high CO oxidation conversion [16]. Noble metal catalysts such as Ru and Rh based on AL_2O_3 are very active and selective at about 100 ℃. While the Pt metal based on Al_2O_3 is similarly very active and selective at the temperature of about 200 ℃ [16, 17].

A purifying system must be used to achieve a high hydrogen purity percentage (above 99%). There are several methods for purifying hydrogen, including cryogenic distillation, membrane separation, and pressure

swing adsorption (PSA) [18, 19]. Among these methods, PSA has become the most widely used separation process for H_2 purification in chemical and petrochemical industries [20]. Impurities in the gas mixture including hydrogen are selectively absorbed on solid meso and micro porous adsorbents (i.e., zeolite, activated carbon, silica, and alumina gel) at high partial pressure. Then the adsorbed components are removed from the adsorbent by reducing the partial pressure of the gas phase so that the absorber can be reused. Ribeiro and colleugues studied the purification of hydrogen from the feed flow mixture, including impurities CO_2, CO, and N_2, by simulating an activated carbon/zeolite adsorbent. Their results obtained hydrogen with a purity of 99.9994% in the output stream from a single-bed column simulation [21].

The focus of the present work is on the design and simulation of the purification system. First, the methanol steam reforming process is explained briefly and then the process is divided into two parts. The first part of section 2 is related to the design and simulation of the PROX reactor to reduce the concentration of carbon monoxide and investigate the effect of operational parameters. Section 2's second part is related to the simulation of the pressure swing adsorption process (PSA) in order to obtain hydrogen with a purity of more than 99.99% and validation of the simulation. Section 3 discusses the results and section 4 states the study conclusions.

2. Steam reforming process and purification system

One method of hydrogen production is methanol steam reforming. In this method, methanol is in liquid form at ambient conditions, which allows for compact storage and transportation of the fuel prior to reformation [22]. Since the output of a methanol-reformer reactor contains a small amount of carbon monoxide, a PROX reactor is generally used as a purification system to reduce the concentration of this component and convert it into carbon dioxide. Next, a PSA system, one of the purification methods, is used to obtain high-purity hydrogen.

2.1 Steam reforming of methanol

$CuO/ZnO/Al_2O_3$ catalysts, which work with an operating temperature in a range of 473-573 K, are used in the methanol steam reforming process. In a simulated methanol steam reforming reactor, the feed contains water and methanol with an S/C ratio of 1-1.4 [23]. Under the right conditions, the most favorable stoichiometric reaction is the steam methanol reforming reaction (SMR). In the SMR process, the presence of methanol and steam along with the catalyst at high temperatures leads to many parallel chemical reactions. In addition to the SMR reaction, there are usually two other reactions that occur during the reforming process: the water-gas reaction (WGS) and the methanol decomposition (MD) reaction. The three main reactions that take place in the methanol steam reformer are shown in the following equations [24].

$$CH_3OH + H_2O \rightarrow CO_2 + H_2 \qquad \Delta H_{298K} = 49.37 \text{ kJ/mol} \qquad (1)$$

$$CH_3OH \rightarrow CO + H_2 \qquad \Delta H_{298K} = 90.47 \text{ kJ/mol} \qquad (2)$$

$$CO + H_2O \rightarrow CO_2 + H_2 \qquad \Delta H_{298K} = -41.10 \text{ kJ/mol} \qquad (3)$$

2.2. Cleaning of CO with PROX Reactor

PROX is a reaction to convert carbon monoxide to carbon dioxide, where CO competes with hydrogen for a reaction with oxygen. Therefore, some oxygen is consumed in this reaction. The catalyst plays an important role in increasing CO oxidation and reducing hydrogen oxidation. Two reactions are taking place at the same time inside the PROX reactor, the oxidation reaction of carbon monoxide as the main reaction and the oxidation reaction of hydrogen as a side reaction

that must be directed so that its effect, which leads to the production of water and hydrogen oxidation, becomes insignificant. PROX reactions are shown in equations (4) and (5) [25].

$CO+1/2O_2 \longrightarrow CO_2$ H=-282.98 kJ/molΔ (4)

$H_2+1/2O_2 \longrightarrow H_2O$ H=-241.82 kJ/molΔ (5)

2.3. Pressure Swing Adsorption Process

Pressure swing adsorption (PSA) is a widely used technology to separate several types of gases from gas mixtures. Because different gases tend to be more or less absorbed on different solid surfaces, adsorbents such as zeolites, activated carbon, molecular sieves, etc., are preferred for the adsorption of gaseous species with high affinity at high pressure [26]. Then the absorbed components are removed by reducing the partial pressure of the gas phase so that the adsorbent can be used again. Activated carbon is the preferred carbon dioxide absorber in the off-gas stream produced by a methane steam reformer unit. For this reason, an active carbon layer is used at the end of the adsorption column. Commercial activated carbon has shown good adsorption and selectivity of carbon dioxide performance in the PSA system [27].

2.4. Model assumptions and equations

The kinetics of the reactions carried out in a PROX reactor based on the Power-low model are given in equations (6) and (7) along with kinetic coefficients and activation energy. The main assumptions in the modeling of the PROX reactor are as follows [13]:

- Ideal gas phase
- Reactor pressure is constant (there is no pressure drop in the system)
- Physical properties such as density, catalyst weight, and specific heat capacity are constant
- No back-mixing occurs in the resulting stream inside the reactors

The oxidation reaction of carbon-monoxide [28]:

$$-r_{co} = k \exp(-E/R_g T)\, P_{CO}^{\alpha}\, P_{O2}^{\beta} \quad (6)$$

$k = 1.4 * 10^8\ m^3/kg_{cat}.s$

$E = 78$ Kj/mol

$\alpha = -0.51$

$\beta = 0.76$

Hydrogen oxidation reaction [[29]:

$$-r_{H2} = k \exp(-E/R_g T)\, P_{O2}^{\alpha} \quad (7)$$

$k = 6.19 * 10^{-5}(mol / s.\ Kg_{cat})$

$E = 21.9$ Kj/mol

$\alpha = 0.804$

The development of the PSA model requires the exact investigation of the following assumptions to simplify the balance of mass, energy, and momentum [30]:

- Ideal gas phase
- There are no radial changes in temperature, pressure, and speed
- Non-isothermal energy balance with conductive heat transfer between gas-solid
- The momentum equation is expressed by Ergun's equation
- Adsorption of components on the adsorbent is based on the dual site Langmuir isotherm model and based on the partial pressure

$$W_i = \frac{IP_{1i^e}\, IP_{2i} / T_s P_i}{1+\sum k\,(IP_{3k^e}\, IP_{4k} / T_s P_k} + - \frac{IP_{5i^e}\, IP_{6i} / T_s P_i}{1+\sum k\,(IP_{7k^e}\, IP_{8k} / T_s P_k} \quad (8)$$

Where P is the total pressure, IP_k is the isotherm parameter for species k, Ts is the wall temperature (which is equal to 303 K), and Wi is the loading components on the absorber.

The mass balance equations for each component and for the total mass of the mixture are given in equations (9) and (10), respectively[30]:

$$-D_L \frac{\partial^2 c_i}{\partial z^2} + \frac{\partial c_i}{\partial t} + u \frac{\partial c_i}{\partial t} + c_i \frac{\partial u}{\partial z} + \rho_p \frac{(1-\varepsilon_{bed})}{\varepsilon_{bed}} \frac{\partial q_i}{\partial t} = 0 \quad (9)$$

$$C\frac{\partial u}{\partial c}+\frac{\partial C}{\partial T}+\rho_p\frac{(1-\varepsilon_{bed})}{\varepsilon_{bed}}+\sum_{i=1}^{n}\frac{\partial q_i}{\partial T}=0 \quad (10)$$

Where c_i is the gas concentration of component i, u is the gas velocity, $\rho_{p\ is}$ the particle density, ε_{bed} is the bed porosity, q_i is the absorbed concentration of component i, C is the total concentration, z is the axial coordinate, and D_L is the axial dispersion coefficient.
D_L is calculated from equation (11) [30]:

$$D_L=0.7D_m+\frac{1}{2}d_p u \quad (11)$$

Where d_p is the particle diameter, and D_m is the molecular permeability obtained from the Chapman–Enskog equation.
The adsorption rate is given by the linear driving force (LDF) model given by Equation (12) [31]:

$$\frac{\partial q_i}{\partial t}=ki\,(q_i^{*}-q_i),i=1,2,3,...,N \quad (12)$$

Where k_i is related to the mass transfer coefficient of components and q_i^* is the loading of component i.
The energy balance equation is expressed as equation (13) with the assumption of thermal balance between gas and solid for the substrate [32]:

$$-k_L\frac{\partial^2 T}{\partial z^2}+(\varepsilon_{bed}cC_{pg}+(1-\varepsilon_{bed})\rho_p C_{ps})\frac{\partial T}{\partial z}=(1-\varepsilon_{bed})\rho_{pg}\sum_{j=1}^{N}\Delta H_j\frac{\partial q_j}{\partial t}+2\frac{h_i}{r_i}(T_w-T) \quad (13)$$

Where K_L is the effective axial thermal conductivity, C_{Pg} and C_{Ps} are the specific heat of gas and solid phase. T_W, h_i, and r_i are the wall temperature, the heat transfer coefficient of the inner column wall, and the inner radius of the column, respectively. ΔHj is the absorbed and released heat of the components.
The equation of energy per unit length is given in equation (14) [32]:

$$\rho_w C_{pw}A_w\frac{\partial T_w}{\partial t}=2\pi r_i h_i(T-T_w)-2\pi r_o h_o(T_w-T_{abm}) \quad (14)$$

Where ρ_w, $C_{pw,}$ and A_w are the density, specific heat, and wall cross-section, respectively. T_{amb} is the ambient temperature, and h_o and r_o are the heat transfer coefficient of the outer column wall and the outer radius of the column wall, respectively.
Ergun's equation has been used to calculate the pressure drop along the bed, which is expressed in equation (15) [30]:

$$-\frac{\partial p}{\partial z}=150\frac{\mu u(1-\varepsilon_{bed})^2}{dp^2\varepsilon_{bed}^{\ 2}}+1.75\frac{\rho_g u^2(1-\varepsilon_{bed})}{dp\,\varepsilon_{bed}} \quad (15)$$

Where ρ_g is the gas bulk density, μ is the gas viscosity, and u is the gas velocity.

2.5 Simulation of Reforming and purification processes

Aspen plus V11.0 software was used to simulate the methanol steam reforming process and cleaning system. Adsorption bed and PSA simulation were done using Aspen Adsorption V11.0 software. To determine the compounds and their properties, the desired components were selected in Aspen properties V11.0 software, and after selecting the components, the components were stored in the list of Aspen adsorption software compounds.

2.5.1 Simulation

In the first step of the simulation, the feed to the reforming system contained water and methanol, with a combined methanol mass flow rate of 1.58 kg/hr, water mass flow rate of 1.25 kg/hr, a molar ratio of 1.4, at 25 °C, and pressure 1 bar entered the reforming tubular reactor. The reformer reactor had an operating temperature of 220°C and geometric conditions including a reactor length of 40.3 cm, diameter of 6 mm, and 55 tubes. The bed reactor was filled with 7.8 gr of Cu/ZnO/Al_2O_3 catalyst, the bulk density of the catalyst was 1234.5 kg/m^3, and the porosity of the bed was 0.5 [23]. The output stream from the methanol steam re-

forming reactor after passing through the condenser with the purpose of cooling and condensing the output stream included 0.3% water, 1.2% methanol, 23% carbon dioxide, about 71.5% hydrogen, and 0.9% carbon monoxide.

Next, the PROX system was used to remove carbon monoxide. As can be seen in Figure 1, first the output flows from the condenser along with pure oxygen (0.0608 kg/hr), at a ratio of O_2/CO = 1.1, entered the mixer at a temperature of 25 °C and a pressure of 1 atmosphere. Then, the output stream from the mixer entered the heater for pre-heating to the reaction temperature of 200.5°C. After heating, the feed entered the PROX reactor. The reactor had a length of 480 mm, an inner diameter of 1.38 mm, consumed 40 gr of catalyst [29] for each reactor tube, and a bed porosity of 0.46 as well as performed reactions kinetics as defined in the PROX reactor simulation section. Since the flow rate of the input feed and the amount of the catalyst were considered for one tube in the simulated PROX reactor, the DIVDER tool was used to consider all pipes (10 pipes). And the total flow was divided by the total number of pipes (10) to divide the flow. In the same way, in the continuation of the simulation, the output flow from the PROX reactor enters only one pipe, so it must be multiplied by the total number of pipes (10) using the MULT10 tool. The simulation of the PROX section is shown in Figure (2).

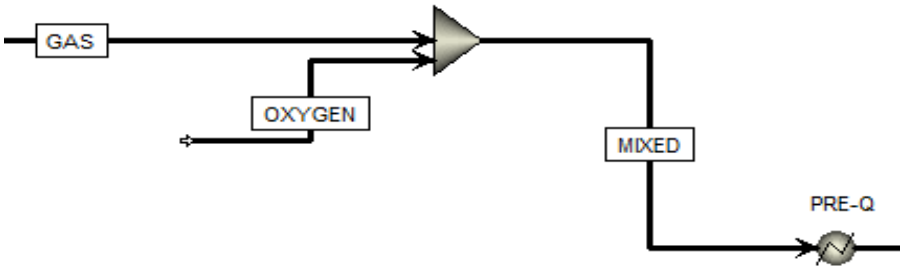

Fig. 1. Simulation of the process up to the pre-heating stage.

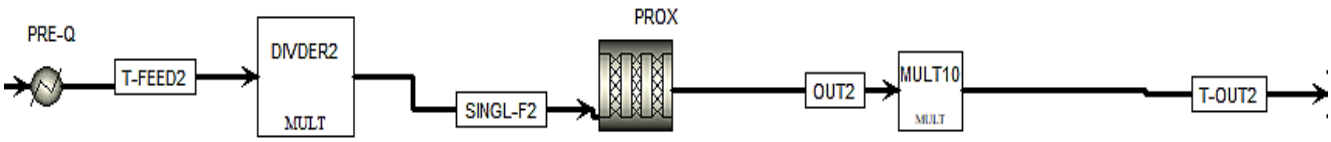

Fig. 2. Process simulation - PROX reactor section.

In the following, to obtain hydrogen with a high purity percentage for fuel cells, the PSA process studied by Abdeljaoued et al. was investigated [30]. In their work, a 4-bed pressure swing adsorption (PSA) process, which is capable of purifying hydrogen from a quaternary mixture (H_2/CO_2/CO/CH_4) obtained from the ethanol steam reforming process, was designed, simulated, and investigated. In our system, the feed contains 73% hydrogen, 23% carbon dioxide, 1% carbon monoxide, and 1% methane. Also, in order to

design and simulate a 4-bed process was investigated. The goal was to produce hydrogen with a purity of 99.99% for a fuel cell. In order to quickly solve the simulation, a "uni-bed" simulation was chosen for modeling. Since this work uses a uni-bed model to simulate the 4-bed process, only the steps of one uni-bed can be modeled. For simplicity, the steps in substrate 1 were chosen. The total cycle time for the 4-bed process is 1600 seconds; the total adsorption time for the 1-bed process is 100 seconds. The dimensions of the column, physical properties of the absorber, general operating conditions in the simulation, parameters of the dual site Langmuir isotherm, Mass coefficients, and heat of adsorption are shown in Tables 1 and 2.

Table 1. Dimensions of columns, physical properties of absorbers, and general operating conditions in the simulation [30].

Parameters	Values
Absorbent	Activated carbon
Bed length, L (cm)	34
Bed diameter, d (cm)	6.4
Particle radius, (mm)	0.601
Feed temperature, (°C)	24.6
Environment temperature, (°C)	25
Feed pressure, (bar)	8.5
Desorption pressure, (bar)	1
Feed flow rate, (mol/s)	0.047742
Particle density, (g/cm^3)	1.969
Buffer volume, (m^3)	3
Gas phase heat conductivity, (W/m/K)	0.104982
Solid-gas heat transfer coefficient, (w/m^2K)	38
Wall-gas heat transfer coefficient, (w/m^2K)	12

Table 2. The parameters of the dual-site Langmuir isotherm, Mass coefficients, and heats of adsorption [30].

Parameters	CO_2	CO	CH_4	H_2
IP1 (Kmol/kg bar)	$3.18.(10^{-3})$	$6.57.(10^{-4})$	$6.57.(10^{-4})$	$2.81.(10^{-5})$
IP2 (K)	0.6456	0.7568	0.7568	0.387
IP3, (1/bar)	0.9059	0.8245	0.8245	$6.12.(10^{-3})$
IP4, (K)	0.4044	0.4041	0.4041	0.4037
IP5, (Kmol/kg bar)	$2.74.(10^{-4})$	$6.2.(10^{-4})$	$6.2.(10^{-4})$	0
IP6, (K)	0.0951	0.0952	0.0952	0.0964
IP7, (1/bar)	0.0651	0.2107	0.2107	0.1320
IP8, (K)	0.9420	0.9421	0.9421	0.9421
K, (1/S)	0.3	0.7	0.5	0.3
ΔH_{ads} , (J/mol)	-30100	-17968	-19678.86	-10494

A schematic diagram of the cycle used in the PSA system is shown in Figure (3).

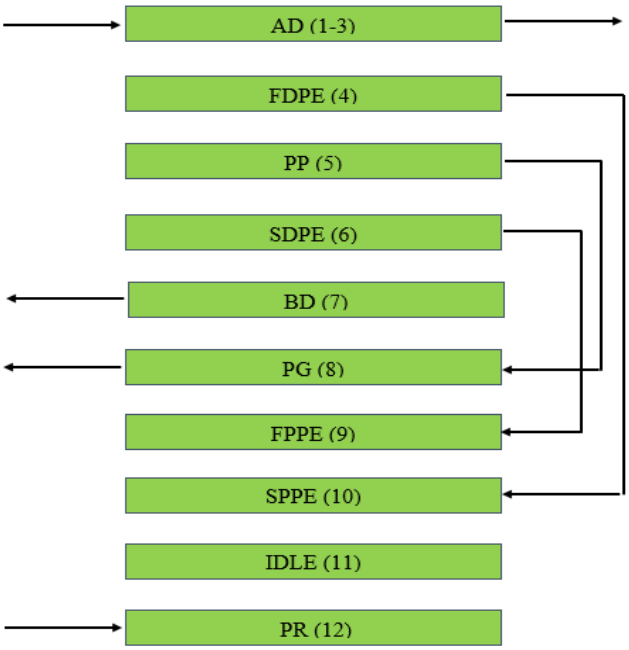

Fig. 3. Schematic diagram of the cycle used in the PSA system [30].

The steps of the cycle for the uni-bed of the PSA process are shown in Table 3.

Table 3. Cycle steps for a uni-bed PSA process.

Step	1	2	3	4	5	6	7	8	9	10	11	12
Bed 1	AD	AD	AD	FDPE	PP	SDPE	BD	PG	FPPE	SPPE	IDLE	PR
Time (s)	1.5	97	1.5	1.5	97	1.5	1.5	94	2.5	9	83.5	11.5

The simulation performed in the software is shown in Fig (4).

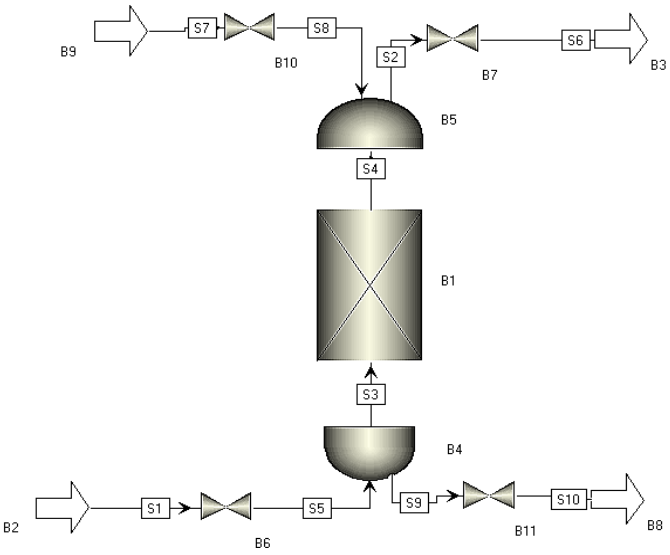

Fig. 4. Simulation performed in the software.

Where B2 is the feed flow, B3 is the Product flow, B9 is the Purge flow, and B8 is the Blow down flow.
The following section describes the cycle or coded program (TASK) that should be used to execute the PSA process according to the stated steps.

3. Results and discussion

The molar fraction changes of the components in the PROX reactor length are shown in Figure (5). According to the reactions carried out in the PROX reactor, the water fraction increased due to the production of water in the hydrogen oxidation reaction, and the amount of hydrogen decreased by a very small amount. Also, due to the oxidation of carbon monoxide, which led to the production of carbon dioxide, the amount of CO_2 increased a little and the amount of output CO rapidly decreased and reached zero at the beginning of the reactor. The results after completing the simulation of the PROX reactor are shown in Table 4 [13]:

Table 4. The results obtained at the output of the PROX reactor.

Components	Single –F2	OUT2
H_2O	0.0300	0.04117
CH_3OH	0.0122	0.01229
CO_2	0.2304	0.2415
H_2	0.7096	0.7050
CO	0.0089	0
O_2	0.0088	0

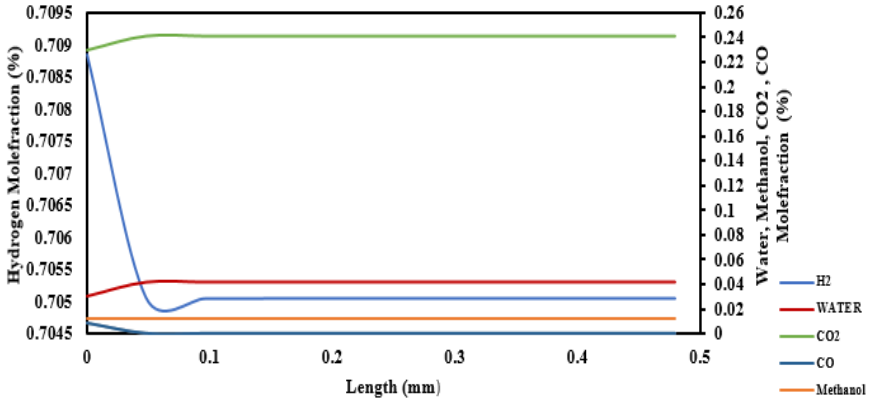

Fig. 5. Changes in the mole fraction of components in the PROX reactor length.

According to the previous section, a PSA system or membrane reactor should be used to obtain hydrogen with a high purity percentage. Considering that more than 85% of hydrogen production units in the world use PSA technology to purify their produced hydrogen and due to its advantages over membrane processes, the PSA process was used in this work. Using this process, water and methanol can be easily condensed and removed from the mixture, which simplified the purification of hydrogen and the removal of other components [9, 12]. One of the key factors in the PSA process is the isotherms related to the adsorption of components on the adsorbent (activated carbon). To obtain the isotherms using the graphs given in the article[30] , a temperature of 30 °C was chosen, which was close to the feed temperature. First the isotherm unit was converted from mol/kg to kmol/kg, so using MATLAB software, w is drawn in terms of P. Next, the isotherm coefficients are obtained using the Curve Fitting tool and the equation given for W. Finally, using the obtained isotherm coefficients, W was obtained. The results are shown in Figure (6).

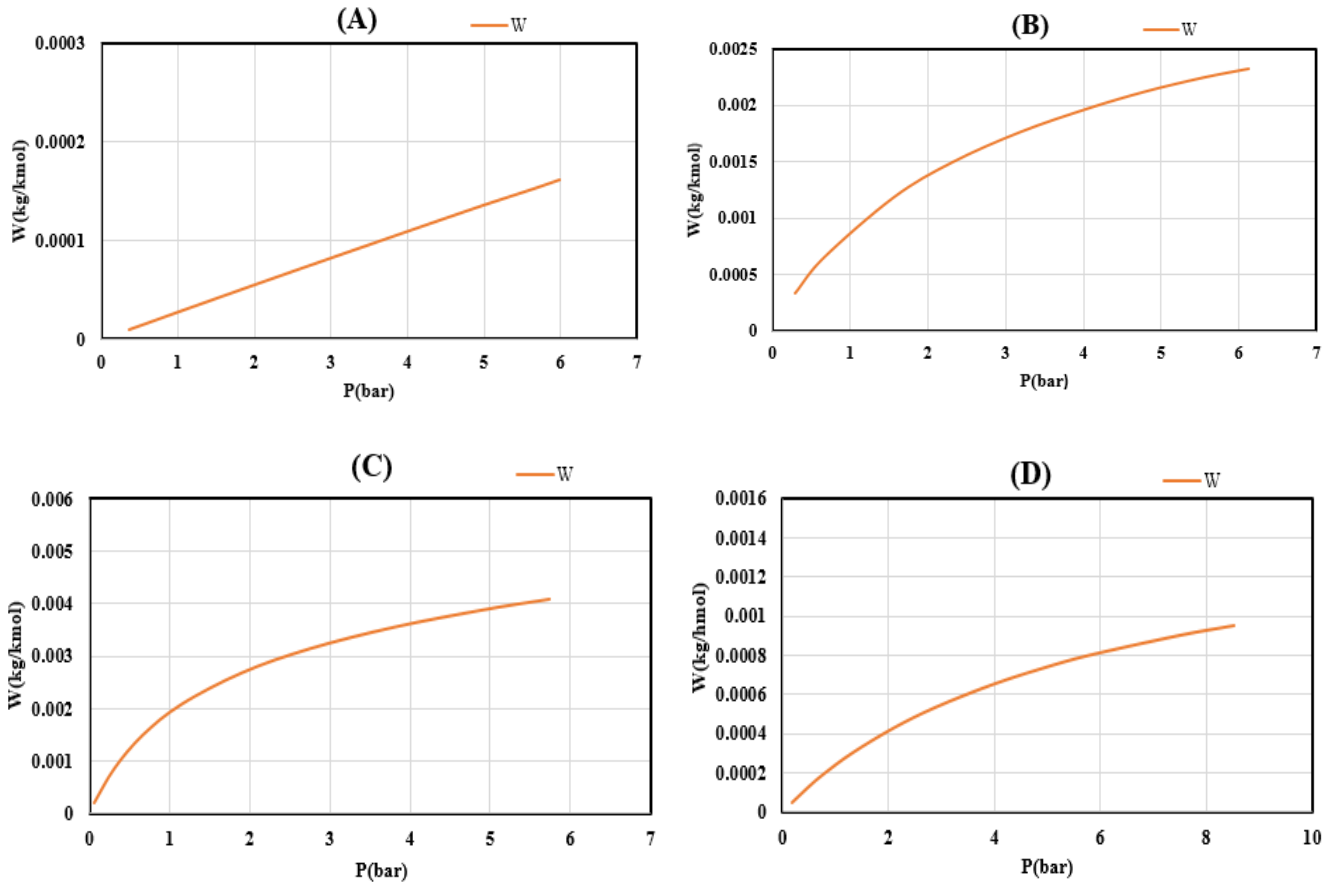

Fig. 6. Diagrams related to isotherms of components: (A): Hydrogen, (B): Methane, (C): Carbon dioxide, (D): Carbon monoxide.

The results obtained from the simulation for pressure changes during one cycle are shown in Figure (7).

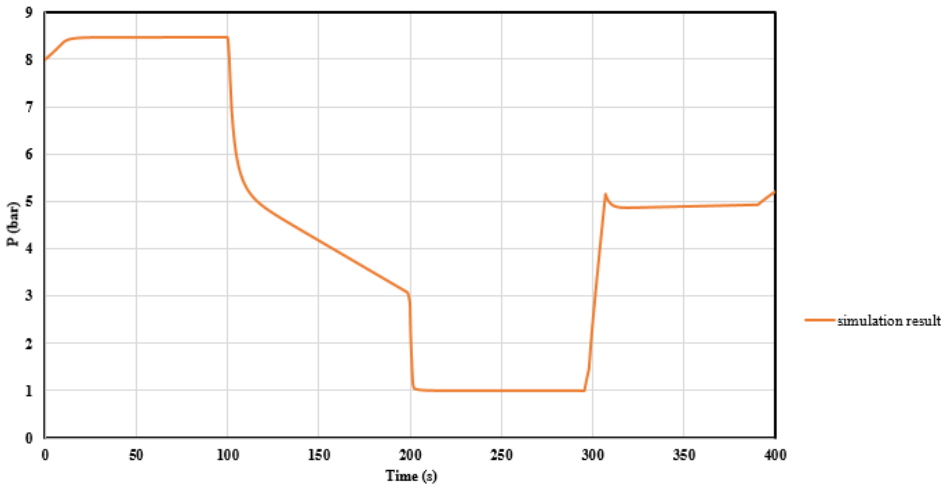

Fig. 7. Pressure changes during one cycle.

The results obtained from the simulation are given in Table 5.

Table 5. Mole fraction of the output components from the PSA column.

Components	Simulation results
CH_4 (ppm)	0.8829
CO (ppm)	83.9052
CO_2 (ppm)	0.1641
H_2 (%)	99.9915

In the following, the results of this study's simulation were compared with Abdeljaoued's results [30] for validation. First, the isotherm diagrams obtained from the simulation used in the Aspen Adsorption software were compared with the diagrams in the article, and the results are shown in Figure (8). According to the figure, there is a good agreement between Abdeljaoued's article and our results, showing that the obtained isotherm parameters are valid [30].

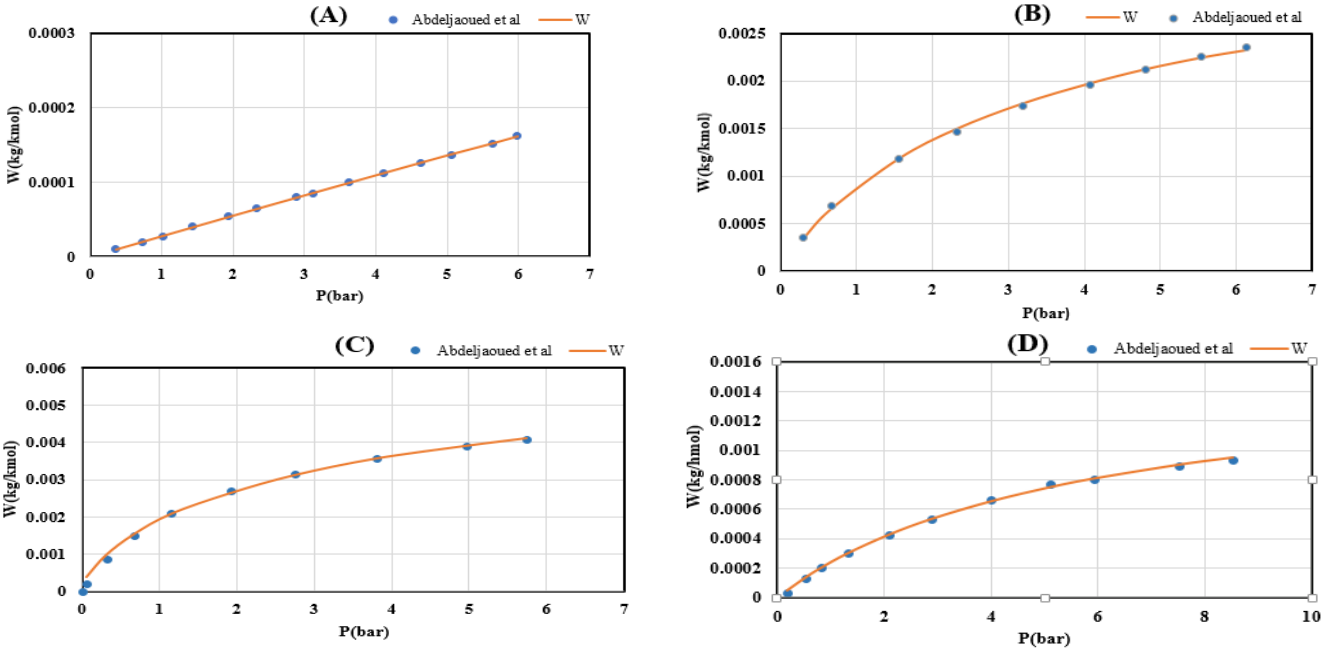

Fig. 7. Validation of isotherm diagrams related to components: A): Hydrogen, (B): Methane, (C): Carbon dioxide, (D): Carbon monoxide.

Also, the further comparison of pressure changes during one cycle is shown in Figure (8), according to the figure there is good agreement between the simulation data and Abdeljaoued's article data [30]:

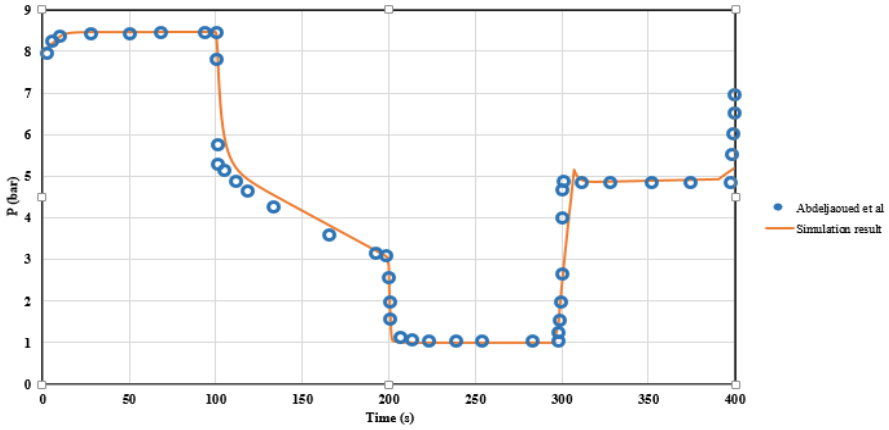

Fig. 8. Validation related to pressure changes over one cycle.

Table 6 shows the simulation results, Abdeljaoued's results (for one cycle), and the calculated error percentage of each component [30].

Table 6. Comparison of simulation results with the results of the article.

Components	Simulation results	Abdel-jaoued et al.	% Error
CH_4 (ppm)	0.08829	0.9	1.9
CO (ppm)	83.9052	84.39	0.57
CO_2 (ppm)	0.1641	0.17	3.45
H_2 (%)	99.9915	99.9913	0.0002

According to the acceptable error percentage between the simulation data and the values obtained from the reference, the performed simulation is valid for use in the methanol steam reforming process as a purifying system.

Conclusion

In the present work, two subsystems were used in the continuation of the methanol steam reforming process. In the first part, the PROX reactor was used as the cleaning method to reduce the concentration of carbon monoxide output from the reformer reactor. A bed reactor filled with Pt/Al_2O_3 catalyst, which led to an increase in the reaction rate, was used to simulate the PROX reactor. The output results from the PROX reactor showed that in the reactor, the molar fraction of carbon monoxide was completely removed from the system, and the molar fraction of hydrogen decreased slightly due to hydrogen oxidation. In the second part, a uni-bed PSA column containing activated carbon adsorbent was designed and simulated as a PSA column for a purifying system to increase the purity of hydrogen up to 99.99%. The process consisted of 12 steps and 4 cycles, the adsorption time was equal to 100 seconds, and the total time of each cycle was about 400 seconds. Hydrogen with a purity of 99.9915% was obtained in the out stream of the PSA column after one cycle. In order to validate the results obtained from the simulation, the present work was compared with Abdeljaoued et al. [30]. The slight difference between our obtained results and the results from this article confirmed the accuracy of the simulation.

Nomenclature

P The total pressure (bar)

IP_k The isotherm parameter for species k

Ts The wall temperature (K)

T_{amb} The ambient temperature

Wi The loading components on the absorber ($Kmolkg^{-1}$)

c_i The gas concentration of component i ($mol\ cm^{-3}$)

C The total concentration ($mol\ cm^{-3}$)

C_{Pg} The specific heat of gas phase ($J\ kg^{-1}\ K^{-1}$)

C_{Ps} The specific heat of gas phase ($J\ kg^{-1}\ K^{-1}$)

C_{pw} The specific heat of wall ($J\ kg^{-1}\ K^{-1}$)

q_i The absorbed concentration of component i ($molkg^{-1}$)

q^*_i The loading of component i ($mol\ kg^{-1}$)

D_L The axial dispersion coefficient ($m^2\ s^{-1}$)

D_m The molecular permeability ($m^2\ s^{-1}$)

d_p The particle diameter (mm)

K_L The effective axial thermal conductivity ($J\ m^{-1}\ K^{-1}s^{-1}$)

k_i The mass transfer coefficient of components (s^{-1})

h_i The heat transfer coefficient of the inner column wall ($W\ m^{-2}$)

h_o The heat transfer coefficient with the outer column wall ($W\ m^{-2}$)

H_{amb} The Solid-gas heat transfer coefficient, (w/m2K)

HTC The Wall-gas heat transfer coefficient, (w/m2K)

r_i The inner radius of the column (cm)

r_o The outer radius of the column wall (cm)

A_w The wall cross-section area (cm^{-2})

z The axial coordinate

L Bed length (cm)

Greek symbols

u The gas velocity ($cm\ s^{-1}$)

ρ_w The density of the wall ($mol\ cm^{-3}$)

ρ_p The particle density ($mol\ cm^{-3}$)

The bed porosity

ΔHj The absorbed and released heat of the components j ($j\ mol^{-1}$)

References

[1] P. Nikolaidis and A. Poullikkas, "A comparative overview of hydrogen production processes," Renewable and sustainable energy reviews, vol. 67, pp. 597-611, 2017.

[2] F. Dawood, M. Anda, and G. Shafiullah, "Hydrogen production for energy: An overview," International Journal of Hydrogen Energy, vol. 45, no. 7, pp. 3847-3869, 2020.

[3] K. Liu, C. Song, and V. Subramani, Hydrogen and syngas production and purification technologies. John Wiley & Sons, 2010.

[4] M. Voldsund, K. Jordal, and R. Anantharaman, "Hydrogen production with CO2 capture," International Journal of hydrogen energy, vol. 41, no. 9, pp. 4969-4992, 2016.

[5] L. Kaiwen, Y. Bin, and Z. Tao, "Economic analysis of hydrogen production from steam reforming process: A literature review," Energy Sources, Part B: Economics, Planning, and Policy, vol. 13, no. 2, pp. 109-115, 2018.

[6] Y. S. Noh, K.-Y. Lee, and D. J. Moon, "Hydrogen production by steam reforming of methane over nickel based structured catalysts supported on calcium aluminate modified SiC," International Journal of Hydrogen Energy, vol. 44, no. 38, pp. 21010-21019, 2019.

[7] S. Xing, C. Zhao, S. Ban, H. Su, M. Chen, and H. Wang, "A hybrid fuel cell system integrated with methanol steam reformer and methanation reactor," International Journal of Hydrogen Energy, vol. 46, no. 2, pp. 2565-2576, 2021.

[8] J. Han, I.-s. Kim, and K.-S. Choi, "Purifier-integrated methanol reformer for fuel cell vehicles," Journal of Power Sources, vol. 86, no. 1-2, pp. 223-227, 2000.

[9] C.-Z. Yao et al., "Effect of preparation method on the hydrogen production from methanol steam reforming over binary Cu/ZrO2 catalysts," Applied Catalysis A: General, vol. 297, no. 2, pp. 151-158, 2006.

[10] A. Kundu, Y. G. Shul, and D. H. Kim, "Methanol reforming processes," in Advances in fuel cells, vol. 1: Elsevier, 2007, pp. 419-472.

[11] T. L. LeValley, A. R. Richard, and M. Fan, "The progress in water gas shift and steam reforming hydrogen production technologies–A review," International Journal of Hydrogen Energy, vol. 39, no. 30, pp. 16983-17000, 2014.

[12] F. Mariño, C. Descorme, and D. Duprez, "Noble metal catalysts for the preferential oxidation of carbon monoxide in the presence of hydrogen (PROX)," Applied Catalysis B: Environmental, vol. 54, no. 1, pp. 59-66, 2004.

[13] M. Ouzounidou, D. Ipsakis, S. Voutetakis, S. Papadopoulou, and P. Seferlis, "A combined methanol autothermal steam reforming and PEM fuel cell pilot plant unit: Experimental and simulation studies," Energy, vol. 34, no. 10, pp. 1733-1743, 2009.

[14] N. Katiyar, S. Kumar, and S. Kumar, "Polymer electrolyte membrane fuel cell grade hydrogen production by methanol steam reforming: a comparative multiple reactor modeling study," Journal of power sources, vol. 243, pp. 381-391, 2013.

[15] O. Laguna et al., "Influence of the O2/CO ratio and the presence of H2O and CO2 in the feedstream during the preferential oxidation of CO (PROX) over a CuOx/CeO2-coated microchannel

reactor," Catalysis Today, vol. 203, pp. 182-187, 2013.

[16] A. Mishra and R. Prasad, "A review on preferential oxidation of carbon monoxide in hydrogen rich gases," Bulletin of Chemical Reaction Engineering & Catalysis, vol. 6, no. 1, p. 1, 2011.

[17] Y. Choi and H. G. Stenger, "Kinetics, simulation and insights for CO selective oxidation in fuel cell applications," Journal of Power Sources, vol. 129, no. 2, pp. 246-254, 2004.

[18] N. Sazali, M. A. Mohamed, and W. N. W. Salleh, "Membranes for hydrogen separation: A significant review," The International Journal of Advanced Manufacturing Technology, vol. 107, no. 3, pp. 1859-1881, 2020.

[19] J. Xiao, Y. Peng, P. Bénard, and R. Chahine, "Thermal effects on breakthrough curves of pressure swing adsorption for hydrogen purification," International Journal of Hydrogen Energy, vol. 41, no. 19, pp. 8236-8245, 2016.

[20] Q. Huang and M. Eić, "Simulation of hydrogen purification by pressure-swing adsorption for application in fuel cells," in Environanotechnology: Elsevier, 2010, pp. 221-244.

[21] A. M. Ribeiro, C. A. Grande, F. V. Lopes, J. M. Loureiro, and A. E. Rodrigues, "A parametric study of layered bed PSA for hydrogen purification," Chemical Engineering Science, vol. 63, no. 21, pp. 5258-5273, 2008.

[22] X. Zhuang, X. Xu, L. Li, and D. Deng, "Numerical investigation of a multichannel reactor for syngas production by methanol steam reforming at various operating conditions," International Journal of Hydrogen Energy, vol. 45, no. 29, pp. 14790-14805, 2020.

[23] A. Chougule and R. R. Sonde, "Modelling and experimental investigation of compact packed bed design of methanol steam reformer," International Journal of Hydrogen Energy, vol. 44, no. 57, pp. 29937-29945, 2019.

[24] J. Zhu, S. S. Araya, X. Cui, S. L. Sahlin, and S. K. Kær, "Modeling and design of a multi-tubular packed-bed reactor for methanol steam reforming over a Cu/ZnO/Al2O3 catalyst," Energies, vol. 13, no. 3, p. 610, 2020.

[25] K. Liu, A. Wang, and T. Zhang, "Recent advances in preferential oxidation of CO reaction over platinum group metal catalysts," ACS catalysis, vol. 2, no. 6, pp. 1165-1178, 2012.

[26] F. V. Lopes, C. A. Grande, and A. E. Rodrigues, "Activated carbon for hydrogen purification by pressure swing adsorption: Multicomponent breakthrough curves and PSA performance," Chemical Engineering Science, vol. 66, no. 3, pp. 303-317, 2011.

[27] T. Keller and G. Shahani, "PSA technology: Beyond hydrogen purification," Chemical Engineering, vol. 123, no. 1, p. 50, 2016.

[28] D. H. Kim and M. S. Lim, "Kinetics of selective CO oxidation in hydrogen-rich mixtures on Pt/alumina catalysts," Applied Catalysis A: General, vol. 224, no. 1-2, pp. 27-38, 2002.

[29] F. Cipitì and V. Recupero, "Design of a CO preferential oxidation reactor for PEFC systems: A modelling approach," Chemical Engineering Journal, vol. 146, no. 1, pp. 128-135, 2009.

[30] A. Abdeljaoued, F. Relvas, A. Mendes, and M. H. Chahbani, "Simulation and experimental results

of a PSA process for production of hydrogen used in fuel cells," Journal of Environmental Chemical Engineering, vol. 6, no. 1, pp. 338-355, 2018.

[31] J. J. Lee, M. K. Kim, D. G. Lee, H. Ahn, M. J. Kim, and C. H. Lee, "Heat-exchange pressure swing adsorption process for hydrogen separation," AIChE journal, vol. 54, no. 8, pp. 2054-2064, 2008.

[32] J. Xiao, R. Li, P. Benard, and R. Chahine, "Heat and mass transfer model of multicomponent adsorption system for hydrogen purification," International Journal of Hydrogen Energy, vol. 40, no. 14, pp. 4794-4803, 2015.